# Understanding the Charge Transport and Polarities in Organic Donor–Acceptor Mixed-Stack Crystals: Molecular Insights from the Super-Exchange Couplings

*Hua Geng, Xiaoyan Zheng, Zhigang Shuai,* Lingyun Zhu, and Yuanping Yi**

In recent years, organic donor (D)–acceptor (A) cocrystals have attracted increasing interest due to the high potential in optoelectronics. Organic D–A binary crystalline systems with 1:1 stoichiometry can be classified into two groups according to their molecular arrangement, either segregated- or mixed-stack systems. Segregated-stack systems forming of separate D and A stacks have been found with high electrical conductivities along the stacking direction[1] or even metallic behaviors at room temperature.[2] However, mixed-stack systems with alternate stacking of D and A molecules generally behave as semiconductors or insulators under ambient conditions. Recently, high luminescence efficiencies were observed for the mixed stacks of naphthalene/TCNB [1,2,4,5-tetracyanobenzene][3] and 4M-DSB [1,4-bis(3,5-dimethylstyryl)benzene]/CN-TFPA [(2Z,2′Z)-3,3′-(1,4-phenylene)bis(2-(3,5-bis(trifluoromethyl) phenyl)acrylonitrile)] complexes.[4] Also, good charge-transport properties and different carrier polarities were reported for a number of D–A mixed-stack materials.[5–11] For instance, a cocrystal composed of a paramagnetic endohedral metallofullerene and a nickel porphyrin was found to show electron mobility up to 0.9 $cm^2 V^{-1} s$ from flash-photolysis time-resolved microwave conductivity measurements.[9] In contrast, organic field-effect transistors based on coronene tetracarboxylate and alkyl viologen derivative nanofibers presented hole-dominant transport behaviors.[10,11] It is noteworthy to mention that remarkable ambipolar transport properties have been observed by theoretical calculations and experimental measurements for some D–A charge-transfer complexes.[4,5,7,8]

Based on a localized charge model, charge transport is not allowed along the stacking direction for the mixed-stack systems, since the nearest-neighbored D or A molecules are too far away to interact directly with each other. In fact, for hole (electron) transport, an effective electronic coupling between adjacent D (A) molecules is manifested by a super-exchange mechanism, where the in-between A (D) molecule acts as bridge. The bridge-mediated electron transfer has been shown to be involved in long distance charge migration in DNA.[12] However, charge transport via super-exchange couplings is rarely reported in organic semiconductors.[5,6] In case that the super-exchange mechanism is dictated by the interaction between the donor HOMO and the adjacent acceptor LUMO, the effective electronic couplings for hole and electron are of the same nature. Consequently, ambipolar charge transport is anticipated.[5] However, for unbalanced and especially unipolar charge transport,[9,10] it will be insufficient when the super-exchange process takes sole account of the HOMO–LUMO interaction.

Here, we investigate the super-exchange couplings by means of a method based on the Larsson partition technique (denoted as partition-based method thereafter).[13] This method can take account of each molecular level of the middle bridge. Furthermore, with respect to the energy-splitting method, it computes effective couplings considering the site energy correction. In order to understand the variety of charge transport polarities, we choose three representative organic D–A mixed-stack crystals (see **Figure 1**), which are calculated to show electron-dominant, hole-dominant, and ambipolar couplings, respectively. Our calculations reveal that the super-exchange charge transport and polarities depend strongly on the energy level alignments and electronic couplings between the adjacent D and A moieties. In addition, structural disorder cannot change the balance of the super-exchange couplings for hole and electron within the thermally accessible region. This work provides the first molecular insight into the electronic couplings for charge transport in organic D–A mixed-stack crystals, paving the way toward rational design of high-performance transporting materials with various charge polarities.

The experimental crystal structures for the studied D–A complexes CHR (chrysene)-TCNQ (7,7,8,8-tetracyanoquinodimethane),[14] PAZ (phenazine)-PMA (pyromellitic dianhydride),[15] and PTZ (phenothiazine)-TCNQ[16] are shown in Figure 1b. The lattice parameters are listed in Table S1, Supporting Information. The CHR-TCNQ and PAZ-PMA crystals belong to triclinic P-1 space group with one D and one A molecule in the conventional unit cell. However, the PTZ-TCNQ crystal is of a monoclinic C2/c space group with four D and four A molecules per unit cell respectively forming four mixed D–A stacks of equivalent structures. As a result of the space group symmetry, the DAD and ADA trimers are centrosymmetric for CHR-TCNQ and PAZ-PMA and rotationally symmetric for PTZ-TCNQ. In consequence, the two D (A) monomers are

Dr. H. Geng, Prof. Y. Yi
Beijing National Laboratory for Molecular Sciences
CAS Key Laboratory of Organic Solids
Institute of Chemistry, Chinese Academy of Sciences
Beijing 100190, China
E-mail: ypyi@iccas.ac.cn
Dr. X. Zheng, Prof. Z. Shuai
MOE Key Laboratory of Organic OptoElectronics and Molecular Engineering
Department of Chemistry, Collaborative Innovation Center of Chemistry for Energy Materials
Tsinghua University
Beijing 100084, China
E-mail: zgshuai@tsinghua.edu.cn
Dr. L. Zhu
National Center for Nanoscience and Technology
Beijing 100190, China

**DOI: 10.1002/adma.201404412**

ADVANCED MATERIALS
www.advmat.de

www.MaterialsViews.com

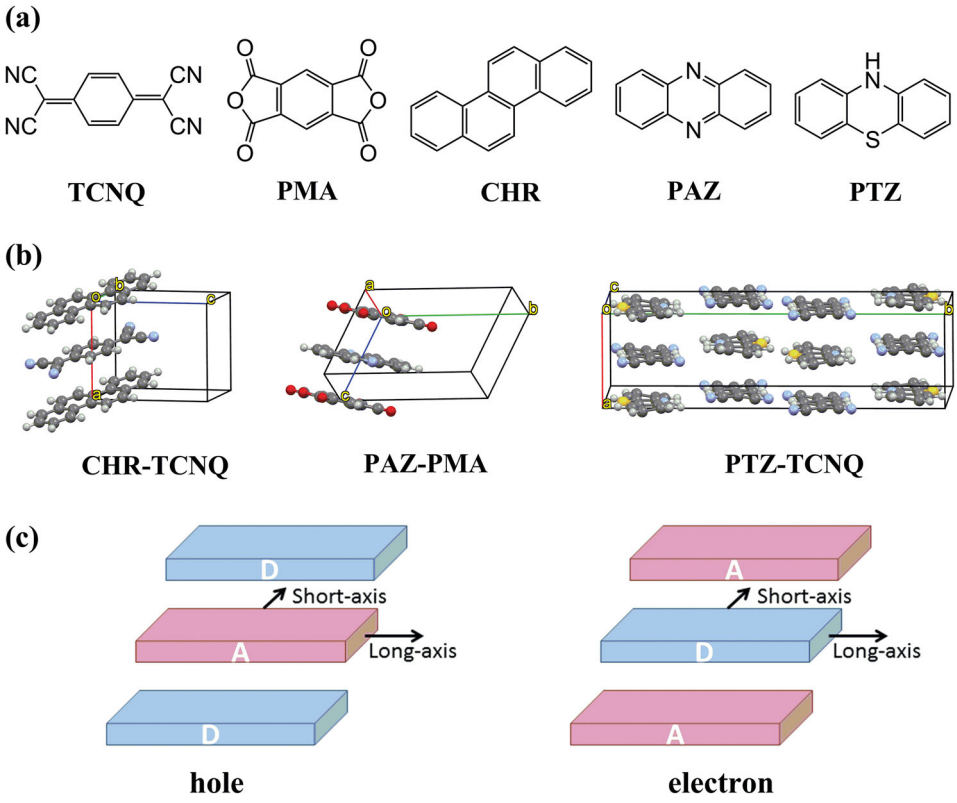


**Figure 1.** a) Chemical structures of two acceptor (upper panel) and three donor moieties (lower panel), b) crystal structures of the studied D–A complexes, and c) schemes of DAD and ADA trimers used for hole and electron super-exchange coupling calculations.

equivalent in presence of the middle A (D) bridge for the DAD (ADA) trimer. As expected, as seen from **Table 1**, the electronic coupling values obtained by the energy-splitting method are almost the same as those by the partition-based method.

Different charge-carrier polarities can be elucidated among the studied systems in terms of the electronic couplings. In the case of CHR-TCNQ, the electronic coupling for hole is vanishingly small, while that for electron can be as large as 50 meV, indicating an excellent electron transport. On the contrary, the PAZ-PMA system exhibits a stronger electronic coupling for hole (ca. 30 meV) than electron (ca. 20 meV). Interestingly, large and equivalent electronic couplings (reaching 70 meV) are found for hole and electron in the PTZ-TCNQ crystal. As a result, remarkable ambipolar charge transport can be anticipated.

To understand the difference in the super-exchange coupling for hole and electron, we seek to assess the role of each bridge level. To this end, we add the bridge orbitals one by one to compute the effective coupling. The effective coupling is composed of two parts: implicit and explicit couplings

$$V^{eff} = V^{im} + \sum_{b\in B} \frac{\tilde{V}_{1b}\tilde{V}_{b2}}{E-\tilde{\varepsilon}_b} \quad (1)$$

The latter is formally decomposed into different terms ascribed to each bridge level. Here, $\tilde{V}_{1b}$ and $\tilde{V}_{b2}$ denote the couplings of the bridge orbital with the frontier orbitals of the two adjacent molecules; $E$ and $\tilde{\varepsilon}_b$ correspond to the energies of the adiabatic and bridge levels in the trimer, respectively. As seen from Figure S1, Supporting Information, the explicit coupling for each bridge level is unaffected irrespective of how many bridge orbitals are considered in calculations. However, the implicit super-exchange coupling can vary dramatically with the number of bridge orbitals (see Figure S2, Supporting Information). The contribution of the $n$th bridge level to the implicit coupling can be estimated as the difference, $V_n^{im} - V_{n-1}^{im}$, where $V_n^{im}$ is the implicit coupling calculated with considering the first $n$ bridge orbitals.

**Figure 2** shows the calculated implicit and explicit couplings for each bridge orbital, as well as the dependence of effective coupling on the number of bridge orbitals. First, we stress that, in the case that none of bridge orbitals is considered, the electronic coupling only contains the implicit part ($V_o^{im}$) and is found to be considerable for electron in CHR-TCNQ and for both hole and electron (they are comparable) in PTZ-TCNQ. Second, for all unoccupied bridge orbitals, the implicit and

**Table 1.** Super-exchange electronic couplings (in meV) for hole and electron transport in the studied D–A mixed-stack crystals.

| | Our method | | Energy-splitting | |
|---|---|---|---|---|
| | Hole | Electron | Hole | Electron |
| CHR-TCNQ | 2 | 47 | 1 | 48 |
| PAZ-PMA | 33 | 21 | 30 | 21 |
| PTZ-TCNQ | 71 | 71 | 68 | 70 |

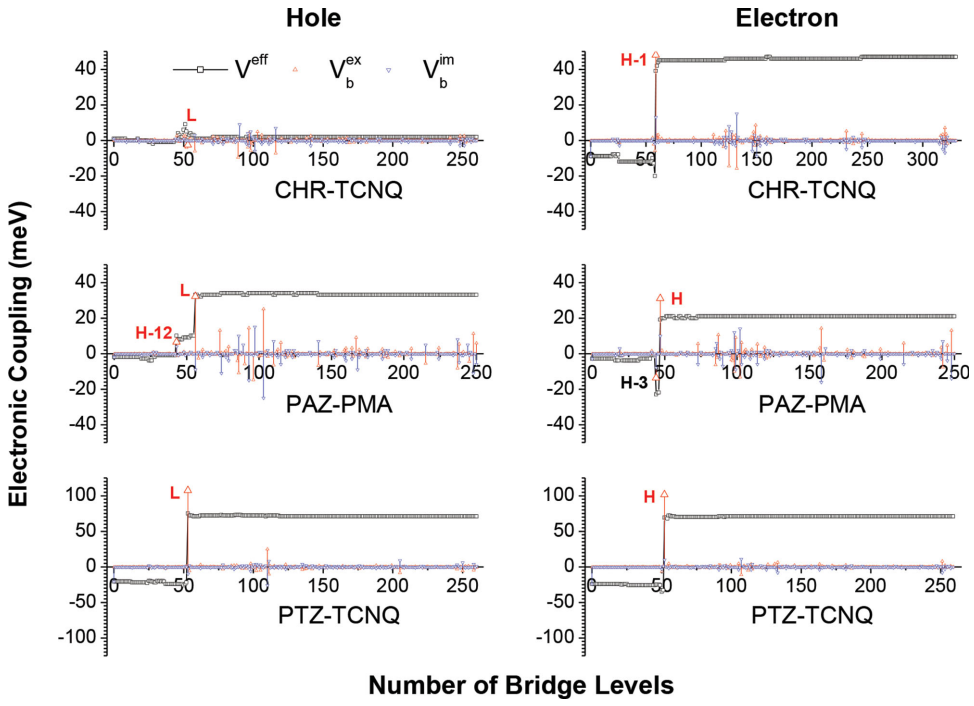


**Figure 2.** Implicit and explicit couplings for each bridge level ($V_b^{im}$ and $V_b^{ex}$), and evolution of effective couplings ($V^{eff}$) as a function of the number of bridge levels.

explicit couplings are of inverse phase. In particular, for the bridge levels above the LUMO, these two counterparts just cancel each other out. The effective coupling is hence converged since adding the LUMO of the bridge. On the contrary, the same trend in the implicit and explicit couplings is found for the occupied bridge orbitals. In general, the implicit term is substantially weaker than the explicit counterpart. Finally, the super-exchange interaction is dominated by a very limited number of essential bridge levels. In the case of PTZ-TCNQ, the electronic couplings for hole and electron are mediated exclusively by the TCNQ LUMO and the PTZ HOMO, respectively. Therefore, the super-exchange interaction is of the same nature for hole and electron, leading to very balanced couplings. For PAZ-PMA, besides the frontier orbital, there is only another appreciable pathway through one occupied orbital of the bridge PMA (PAZ) molecule that plays a constructive (destructive) role for hole (electron). Hence, the electronic coupling for hole is relatively stronger than electron. In contrast, for CHR-TCNQ, the CHR HOMO and the TCNQ LUMO play a negligible bridging role in the super-exchange interaction. Moreover, only the HOMO-1 of the CHR bridge can mediate a significant coupling for electron. Thus, a unipolar coupling is achieved for electron.

We notice that, the original McConnell super-exchange theory only considered the virtual orbitals as bridge in the intramolecular electron transfer between two phenyl groups which are connected by saturated alkyl chains.[17] This assumption might be reasonable, since the occupied orbitals of the alkyl groups are too deep to be accessed by the LUMO of the phenyl groups. In fact, the energy band gap of an organic $\pi$-conjugated molecule is much smaller than that of a saturated alkyl chain. Especially, for the D–A mixed-stack systems, the acceptor LUMO is usually lying close to or even below the donor HOMO. Due to the decreased energy gap, the acceptor LUMO [donor HOMO] has more opportunities to interact with the donor occupied [acceptor unoccupied] orbitals. As seen in Figure 2, if only considering occupied orbitals as bridge for hole transfer or virtual orbitals as bridge for electron transfer, the essential feature of the super-exchange coupling would not exist at all. Thus, for D–A mixed-stack systems, the partition-based method becomes crucial to evaluate the super-exchange couplings due to its capability to take all bridge orbitals into consideration. This is similar to the case that electron is transferred between two metal centers through a molecule as described by Larsson.[18]

According to Equation (1), the main source of super-exchange interaction (the explicit part) depends quadratically on the coupling of the bridge orbital with the transport level of its two adjacent molecules, while is inversely proportional to the energy difference ($\Delta E$) between $E$ and $\tilde{\varepsilon}_b$. Interestingly, as shown in **Figure 3**, $\Delta E$ is linearly dependent on the orbital energy offset between the isolated donor and acceptor, in spite of apparent discrepancy due to polarization effect in the trimer. Accordingly, the role of different bridge orbitals can be correlated to the energy level alignment between the donor and acceptor molecules (see Figure 3). The HOMO–LUMO gaps are in the range from 2.6 to 4.6 eV for all donor and acceptor moieties. In the case of TCNQ and PTZ, the HOMO level is relatively far (ca. 1.8 eV) away from other occupied levels. This will make the HOMO–LUMO interaction greatly superior to other pathways for the electronic coupling in the PTZ-TCNQ crystal. In contrast, for the CHR, PMA, and PAZ moieties, the

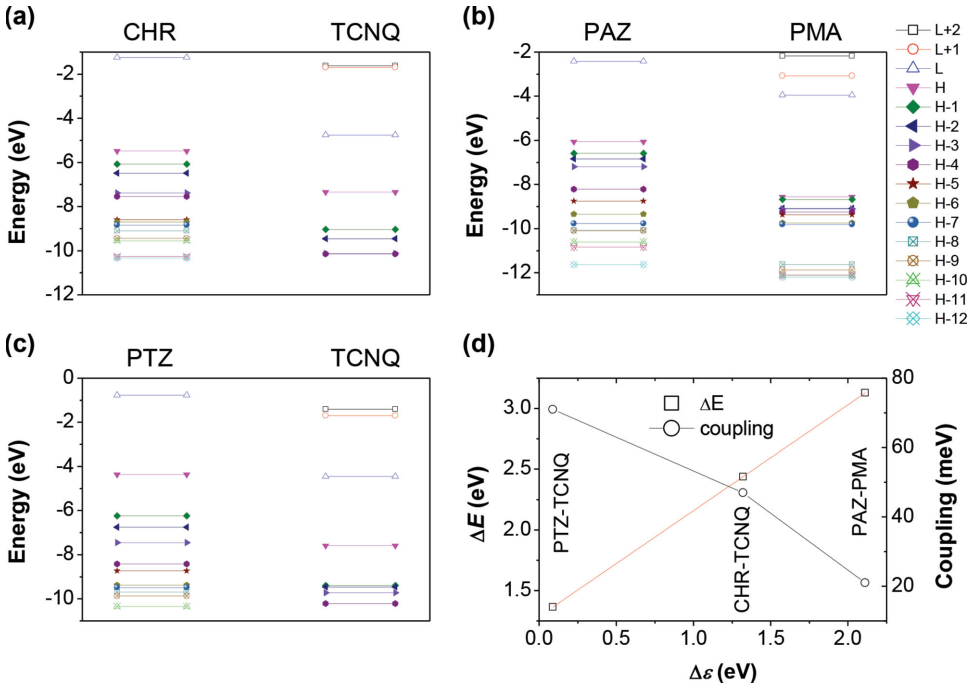


**Figure 3.** a–c) Energy level alignments for the studied systems, and d) dependence of the energy difference ($\Delta E$) between the adiabatic and bridge levels in the trimer and the super-exchange coupling for electron on the orbital energy offset ($\Delta\varepsilon$) of isolated donor and acceptor.

occupied levels display very dense distribution and are close to the HOMO level, so that there are more opportunities to arouse the super-exchange interaction for the electron coupling in the CHR-TCNQ crystal and for both electron and hole couplings in the PAZ-PMA crystal. Namely, the effective couplings for hole and electron can be from different pathways and tend to lose balance, especially for CHR-TCNQ due to lack of the interaction between the donor HOMO and the acceptor LUMO, the common ingredient for hole and electron transport.

To analyze the relative importance of different super-exchange pathways, we need further to compare the electronic couplings of the bridge orbitals with the transport levels of adjacent molecules. It can be seen from **Table 2**, for the studied system, the electronic couplings of the bridge with the two adjacent molecules display a same strength due to the symmetry. The electronic couplings for the essential bridge orbitals are very strong, with the largest absolute values >300 meV. This can be ascribed to a synergistic effect for the donor and acceptor wavefunctions overlaps at different positions (see Figure S3, Supporting Information). In contrast, the couplings for other bridge orbitals with similar energy difference $\Delta E$ are much smaller. For instance, the electronic coupling between the CHR HOMO and the TCNQ LUMO is merely one fifth of the largest value, because the orbital overlaps almost compensate each other in the lateral direction for the CHR-TCNQ dyad as shown in Figure S3, Supporting Information. In a word, the super-exchange couplings will be controlled by only one or two essential bridge orbitals. In addition, the largest D–A couplings are very similar for the three systems; the smaller energy difference, the stronger resulting effective coupling (see Figure 3d).

In order to shed some light on the influence of dynamic structural disorder on the charge-transport properties, we have investigated the dependence of transfer integrals on molecular displacements, which is shown in **Figure 4**. Displaced trimer configurations are constructed from the experimental crystal packing structures by shifting the middle bridge moiety along

**Table 2.** Electronic couplings (in meV) of the donor HOMO/acceptor LUMO with the acceptor/donor bridge orbitals for hole/electron transport (H: HOMO, L: LUMO).

| System | Coupling | Hole | | | Electron | | | |
|---|---|---|---|---|---|---|---|---|
| | | L | H | H-12 | L | H | H-1 | H-3 |
| CHR-TCNQ | $V_{1B}$ | 66 | –59 | 1 | –87 | 72 | 335 | –89 |
| | $V_{B2}$ | 66 | 59 | 1 | 87 | 72 | 335 | 89 |
| PAZ-PMA | $V_{1B}$ | –312 | –13 | 185 | 29 | 309 | –18 | 242 |
| | $V_{B2}$ | 312 | –13 | 185 | –29 | 309 | –18 | –242 |
| PTZ-TCNQ | $V_{1B}$ | –367 | 53 | 31 | –12 | –353 | –72 | 53 |
| | $V_{B2}$ | 367 | 53 | –31 | 12 | –353 | –72 | –53 |

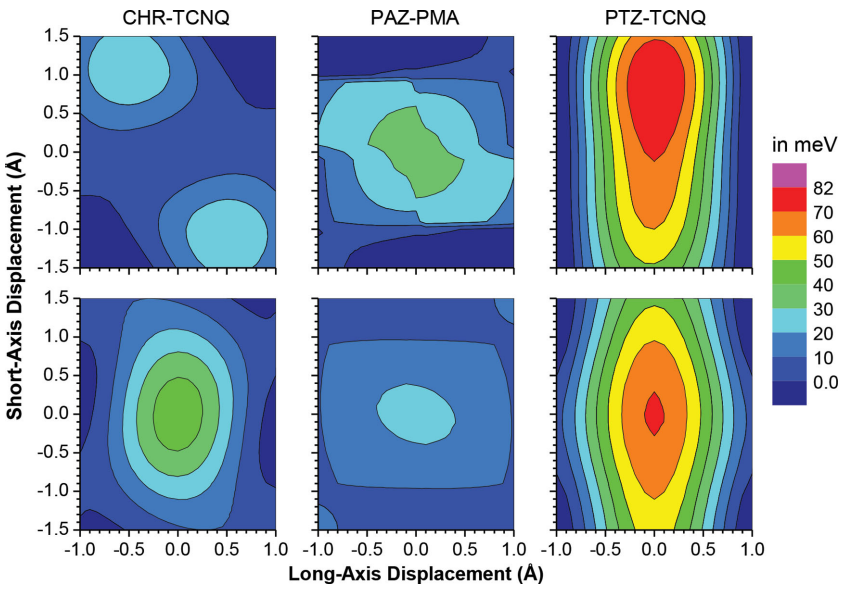


**Figure 4.** Dependence of electronic couplings for hole (upper panels) and electron (lower panels) as a function of displacements along the molecular long and short axes of the bridge (stacking schemes shown in Figure 1c).

its long and short axes while keeping the two neighboring molecules fixed (see Figure 1c). Due to inequivalence of the two D [A] molecules in displaced DAD or ADA trimers, the polarization from neighboring molecules could result in substantial site energy difference between the D [A] molecules. Consequently, the energy-splitting method is no longer applicable. As seen in Figure S4, Supporting Information, and Figure 4, with increasing displacements of the bridge molecule, the energy-splitting method calculated transfer integrals will deviate dramatically from those obtained by the partition-based method.

Consistent with the symmetries of the experimental trimer configurations, the evolutionary patterns for electronic couplings are of inversion symmetry for CHR-TCNQ and PAZ-PMA and of mirror symmetry for PTZ-TCNQ. Overall, all the electronic couplings but the hole coupling for CHR-TCNQ are decreased when the trimer configuration moves away from the experimental structure at the origin. Owing to distinct essential super-exchange pathways, the electronic couplings for hole and electron show different evolution trends, especially for CHR-TCNQ. However, due to the dominant HOMO-LUMO super-exchange nature, similar trends are found for electron and hole in the PTZ-TCNQ system. In general, the fluctuations in electronic couplings for hole and electron due to structural disorder are well correlated to the coupling strengths; the stronger coupling, the larger fluctuation. Interestingly, it is found that the minimums of the total trimer energies for these three systems are located at or near the origin position, corresponding to the crystal structures (see Figure S5, Supporting Information). Within the thermally accessible region, the variance in transfer integral is moderate for CHR-TCNQ (<10 meV) and PTZ-TCNQ (<20 meV), while can be somewhat more significant along the short axis for the PAZ-PMA system. By and large, the charge-transport polarities for the studied systems seem to be unchanged by structural disorder within the thermally accessible range. Here, we would note that the internal reorganization energies cannot modify the charge polarities either (see Supporting Information for more details). However, to gain a deep understanding of the impact of dynamical disorder on the charge-transport properties would require a more detailed investigation of the electron (hole)-phonon coupling interactions.[19]

To summarize, we have investigated the super-exchange electronic couplings for charge transport in three typical organic D–A mixed-stack crystals by means of the partition-based method. Our calculated results show that, generally, all the unoccupied molecular orbitals except the LUMO of the bridge hardly contribute to the electronic couplings for both hole and electron transport. Balanced electronic couplings between hole and electron can be achieved when the coupling is dominated by the interaction between the donor HOMO and the acceptor LUMO. Otherwise, involvement of other bridge orbitals will lead to inequivalent super-exchange couplings, even to unipolar transport in the special case that the interaction between the donor HOMO and the acceptor LUMO vanishes. In addition, the balance of the super-exchange couplings for hole and electron seems unaffected by structural disorder within the thermally accessible region. Our computational results provide helpful insight for rational design of D–A mixed-stack materials with high charge-transport performance and various charge-carrier polarities.

## Experimental Section

The super-exchange charge-transport properties of several D–A mixed-stack systems in recent experimental studies were reasonably explained either by us or by others through computational studies using the energy splitting method.[4,7] However, this method is only applicable in very limited case. When the two monomers in a dimer are not equivalent, the electronic coupling obtained by the energy-splitting method has been demonstrated qualitatively incorrect due to polarization effect.[20] In the case of two-component crystals with mixed-stack donor and acceptor, the polarization effect can be even stronger. On the other hand, the energy-splitting method cannot clarify the role each bridge level can play in the super-exchange charge-transfer process. In contrast to the direct through-space electronic couplings between two adjacent molecules, super-exchange electronic couplings can be derived by calculations based on a bridge-mediated triad (Molecule 1 – Bridge – Molecule 2). For hole transport, bridge, and molecules 1 and 2 denote acceptor and donor, respectively, and vice versa for electron transport (see Figure 1c). The electronic properties of the above triad systems can be described by the following secular equation

$$HC = ESC \tag{2}$$

where $H$ and $S$ are the system Hamiltonian and overlap matrices. After projection to the localized orbitals on the bridge molecule and molecules 1 and 2, we obtain

$$H = \begin{pmatrix} \varepsilon_1 & V_{12} & V_{1B} \\ V_{21} & \varepsilon_2 & V_{2B} \\ V_{B1} & V_{B2} & \varepsilon_B \end{pmatrix} \quad (3)$$

$$S = \begin{pmatrix} 1 & S_{12} & S_{1B} \\ S_{21} & 1 & S_{2B} \\ S_{B1} & S_{B2} & 1 \end{pmatrix} \quad (4)$$

The matrix elements in Equations (3) and (4) can be computed as follows

$$\varepsilon_i = \langle \psi_i | H | \psi_i \rangle \quad (5)$$

$$V_{ij} = V_{ji} = \langle \psi_i | H | \psi_j \rangle \quad (6)$$

$$S_{ij} = S_{ji} = \langle \psi_i | \psi_j \rangle \quad (7)$$

Here, $\psi_{i/j}$ denotes the cluster orbitals localized on molecule 1 or 2 or the bridge molecule, which are constructed using respective isolated molecular orbitals. For hole [electron] transport, $\psi_1$ and $\psi_2$ are the HOMO [LUMO] of D1 and D2 [A1 and A2], respectively, and $\psi_B$ represent the molecular orbitals of the bridge A [D] molecule. The Hamiltonian based on an orthogonalized basis can be then obtained by means of Löwdin's symmetric transformation[21]

$$\tilde{H} = S^{-1/2} H S^{-1/2} = \begin{pmatrix} \tilde{\varepsilon}_1 & \tilde{V}_{12} & \tilde{V}_{1B} \\ \tilde{V}_{21} & \tilde{\varepsilon}_2 & \tilde{V}_{2B} \\ \tilde{V}_{B1} & \tilde{V}_{B2} & \tilde{\varepsilon}_B \end{pmatrix} \quad (8)$$

Here, we note that doing such basis orthogonalization results in polarization effect coherently considered. Next, utilizing Larsson partition technique in connection with perturbation scheme,[13,18] we obtain the effective Hamiltonian matrix by the following equation, in which the bridge states are reduced to the initial and final states in the electron-transfer process

$$\begin{aligned} H^{eff} &= \begin{pmatrix} \varepsilon_1^{eff} & V_{12}^{eff} \\ V_{21}^{eff} & \varepsilon_2^{eff} \end{pmatrix} \\ &= \begin{pmatrix} \tilde{\varepsilon}_1 & \tilde{V}_{12} \\ \tilde{V}_{21} & \tilde{\varepsilon}_2 \end{pmatrix} + \begin{pmatrix} \tilde{V}_{1B} \\ \tilde{V}_{2B} \end{pmatrix} \frac{1}{E - \tilde{E}_B} \left( \tilde{V}_{B1} \tilde{V}_{B2} \right) \end{aligned} \quad (9)$$

where $\tilde{V}_{1B}$, $\tilde{V}_{2B}$, $\tilde{V}_{B1}$, and $\tilde{V}_{B2}$ are vectors, and $\tilde{E}_B$ is matrix. The parameter $E$ is an eigenvalue of the above matrix (in our calculations, $E$ takes the lower eigenvalue for holes but the higher one for electrons), and can be determined by an iterative procedure. Finally, it will converge to one of the adiabatic energies. After diagonalization of the bridge block Hamiltonian matrix, effective electronic coupling can be expressed as

$$\begin{aligned} V_{12}^{eff} &= \tilde{V}_{12} + \sum b \in B \frac{\tilde{U}_b^{+} \tilde{V}_{1B} \tilde{V}_{B2} \tilde{U}_b}{\tilde{U}_b^{+} \left( E - \tilde{E}_B \right) \tilde{U}_b} \\ &= \tilde{V}_{12} + \sum_{b \in B} \frac{\tilde{V}_{1b} \tilde{V}_{b2}}{E - \tilde{\varepsilon}_b} \end{aligned} \quad (10)$$

Here, $\tilde{\varepsilon}_b$ and $\tilde{U}_b$ are the eigenvalues and eigenvectors of the block matrix $\tilde{E}_B$, respectively. From Equation (10), the effective super-exchange coupling consists of two parts, corresponding to the implicit and explicit couplings in Equation (1).

In our calculations, the geometrical structures for the D and A moieties and the DAD and ADA trimers were extracted from the experimental crystal structures. Based on these geometries, molecular orbital energies and coefficients for the monomers and trimers were obtained by density functional theory (DFT) at the B3LYP/6–31G** level, as the resulting super-exchange coupling is insensitive to the choice of functionals (see Supporting Information for more details).[5]

## Supporting Information

Supporting Information is available from the Wiley Online Library or from the author.

## Acknowledgements

This work is supported by National Natural Science Foundation of China (Grant Nos. 21303213, 21373229, 21290191, and 21473043), the 973 Program of the Ministry of Science and Technology of China (Grant Nos. 2011CB932304, 2011CB808405, 2013CB933503, and 2014CB643506), and the Strategic Priority Research Program of the Chinese Academy of Sciences (Grant No. XDB12020200). The numerical calculations have been done in the CNIC supercomputer center of the Chinese Academy of Sciences and the Tsinghua University Supercomputer Center.

Received: September 24, 2014
Revised: November 19, 2014
Published online: January 14, 2015

[1] a) J. Zhang, J. Tan, Z. Ma, W. Xu, G. Zhao, H. Geng, C. A. Di, W. Hu, Z. Shuai, K. Singh, D. Zhu, *J. Am. Chem. Soc.* **2013**, *135*, 558; b) H. Hayashi, W. Nihashi, T. Umeyama, Y. Matano, S. Seki, Y. Shimizu, H. Imahori, *J. Am. Chem. Soc.* **2011**, *133*, 10736.
[2] a) H. Alves, A. S. Molinari, H. Xie, A. F. Morpurgo, *Nat. Mater.* **2008**, *7*, 574; b) M. Sing, U. Schwingenschlögl, R. Claessen, P. Blaha, J. M. P. Carmelo, L. M. Martelo, P. D. Sacramento, M. Dressel, C. S. Jacobsen, *Phys. Rev. B* **2003**, *68*, 125111.
[3] Y.-L. Lei, Y. Jin, D.-Y. Zhou, W. Gu, X.-B. Shi, L.-S. Liao, S.-T. Lee, *Adv. Mater.* **2012**, *24*, 5345.
[4] S. K. Park, S. Varghese, J. H. Kim, S.-J. Yoon, O. K. Kwon, B.-K. An, J. Gierschner, S. Y. Park, *J. Am. Chem. Soc.* **2013**, *135*, 4757.
[5] L. Zhu, Y. Yi, Y. Li, E.-G. Kim, V. Coropceanu, J.-L. Brédas, *J. Am. Chem. Soc.* **2012**, *134*, 2340.
[6] a) L. Zhu, Y. Yi, A. Fonari, N. S. Corbin, V. Coropceanu, J.-L. Brédas, *J. Phys. Chem. C* **2014**, *118*, 14150; b) V. Coropceanu, H. Li, P. Winget, L. Zhu, J.-L. Brédas, *Annu. Rev. Mater. Res.* **2013**, *43*, 63; c) V. Coropceanu, Y. Li, Y. Yi, L. Zhu, J.-L. Brédas, *MRS Bull.* **2013**, *38*, 57.
[7] a) J. Zhang, H. Geng, T. S. Virk, Y. Zhao, J. Tan, C. A. Di, W. Xu, K. Singh, W. Hu, Z. Shuai, Y. Liu, D. Zhu, *Adv. Mater.* **2012**, *24*, 2603; b) Y. Qin, J. Zhang, X. Zheng, H. Geng, G. Zhao, W. Xu, W. Hu, Z. Shuai, D. Zhu, *Adv. Mater.* **2014**, *26*, 4093.
[8] a) T. Wakahara, P. D'Angelo, K. I. Miyazawa, Y. Nemoto, O. Ito, N. Tanigaki, D. D. C. Bradley, T. D. Anthopoulos, *J. Am. Chem. Soc.* **2012**, *134*, 7204; b) H.-D. Wu, F.-X. Wang, Y. Xiao, G.-B. Pan, *J. Mater. Chem. C* **2013**, *1*, 2286.
[9] S. Sato, H. Nikawa, S. Seki, L. Wang, G. Luo, J. Lu, M. Haranaka, T. Tsuchiya, S. Nagase, T. Akasaka, *Angew. Chem. Int. Ed.* **2012**, *51*, 1589.
[10] A. A. Sagade, K. V. Rao, U. Mogera, S. J. George, A. Datta, G. U. Kulkarni, *Adv. Mater.* **2013**, *25*, 559.

[11] A. A. Sagade, K. Venkata Rao, S. J. George, A. Datta, G. U. Kulkarni, *Chem. Commun.* **2013**, *49*, 5847.
[12] C. Murphy, M. Arkin, Y. Jenkins, N. Ghatlia, S. Bossmann, N. Turro, J. Barton, *Science* **1993**, *262*, 1025.
[13] S. Larsson, *Adv. Quantum Chem.* **2002**, *41*, 9.
[14] P. J. Munnoch, J. D. Wright, *J. Chem. Soc., Perkin Trans. 2* **1974**, 1397.
[15] N. Karl, W. Ketterer, J. J. Stezowski, *Acta Cryst. B* **1982**, *38*, 2917.
[16] H. Kobayashi, *Acta Cryst. B* **1974**, *30*, 1010.
[17] H. M. McConnell, *J. Chem. Phys.* **1961**, *35*, 508.
[18] S. Larsson, *J. Am. Chem. Soc.* **1981**, *103*, 4034.
[19] L. J. Wang, Q. Peng, Q. K. Li, Z. Shuai, *J. Chem. Phys.* **2007**, *127*, 044506.
[20] a) E. F. Valeev, V. Coropceanu, D. A. da Silva Filho, S. Salman, J.-L. Brédas, *J. Am. Chem. Soc.* **2006**, *128*, 9882; b) V. Coropceanu, J. Cornil, D. A. da Silva Filho, Y. Olivier, R. Silbey, J.-L. Brédas, *Chem. Rev.* **2007**, *107*, 926.
[21] P. O. Löwdin, *J. Chem. Phys.* **1950**, *18*, 365.